Promoter orientation within an AAV-CRISPR vector affects Cas9 expression and gene editing efficiency

Running Title: Promoter orientation in AAV-CRISPR vectors

Authors:
Lewis E. Fry[1,2*], Caroline F. Peddle[1], Marta Stevanovic[1], Alun R. Barnard[1,2], Michelle E. McClements[1] and Robert E. MacLaren[1,2]

[1] Nuffield Laboratory of Ophthalmology, Nuffield Department of Clinical Neurosciences & NIHR Oxford Biomedical Research Centre, University of Oxford, Oxford, United Kingdom.
[2] Oxford Eye Hospital, Oxford University Hospitals NHS Foundation Trust, Oxford, United Kingdom.

***** Correspondence: enquiries@eye.ox.ac.uk
Mailing Address: Nuffield Department of Clinical Neuroscience, Level 6, West Wing, John Radcliffe Hospital, Oxford, United Kingdom OX3 9DU

Journal
The CRISPR Journal

Funding:
This research was funded by support from the NIHR Oxford Biomedical Research Centre, the Rhodes Trust, the North Harbour Club Charitable Trust and the Amar-Franses & Foster-Jenkins Trust.

Key words
Cas9, Gene therapy, AAV, Transcription, Viral Vector

Author Contributions
L.E.F. design of experiments, data acquisition, analysis and interpretation, drafting of manuscript. C.F.P. design of experiments, data acquisition, analysis and interpretation, editing and review of manuscript. M.S. data acquisition, analysis and interpretation, editing and review of manuscript. A.R.B. data interpretation, editing and review of manuscript. M.E.M. design of experiments, data acquisition and interpretation, editing and review of manuscript. R.E.M. study conception and design, data interpretation, editing and review of manuscript.

All co-authors have reviewed and approved of the manuscript prior to submission.

The manuscript has been submitted solely to this journal and is not published, in press, or submitted elsewhere.

Competing Interests
The authors have no competing financial interests to declare. The funders had no role in the design of the study; in the collection, analyses, or interpretation of data; in the writing of the manuscript, or in the decision to publish the manuscript.

Abstract

Adeno-associated viral vectors have been widely adopted for delivery of CRISPR-Cas components, especially for therapeutic gene editing. For a single vector system, both the Cas9 and guide RNA are encoded within a single transgene, usually from separate promoters. Careful design of this bi-cistronic construct is required due to the minimal packaging capacity of AAV. We investigated how placement of the U6 promoter expressing the gRNA on the reverse strand to SaCas9 driven by a CMV promoter affected gene editing rates compared to placement on the forward strand. We show that orientation in the reverse direction reduces editing rates from an AAV vector, due to reduced transcription of both SaCas9 and guide RNA. This effect was only observed following AAV transduction, but not plasmid transfection. These results have implications for the design of AAV-CRISPR vectors, and suggest results from optimising plasmid transgenes may not translate when delivered via AAV.

Introduction

Adeno-associated viral (AAV) vector delivery of CRISPR-Cas9 is a promising approach for gene editing of somatic tissues *in vivo*.[1] AAV vectors have been used across a range of clinical gene therapy trials for efficient and safe transgene delivery.[2–4] The CRISPR-Cas9 system can be packaged in AAV and has been used to edit genes in the liver,[5–8] retina,[1,9–12] brain,[13] heart[14,15] and skeletal muscle[16–18] in animal models.

For clinical translation, packaging both the Cas9 and guide RNA (gRNA) in a single AAV-CRISPR vector is ideal. This approach requires a bi-cistronic vector design, where both the Cas9 and gRNA components are packaged together with their respective promoters within the limited capacity of a single AAV (~4.7kb). Achieving optimal expression of Cas9 and gRNA is important to maximise on-target editing efficiency and minimise the required vector dose to be delivered. While the arrangement of expression cassettes within a bi-cistronic construct can affect expression of one or both of the transgenes,[19–23] little is known about how vector design affects Cas9 and gRNA expression in a single AAV system.

Authors have noted that the orientation of the U6-gRNA transcriptional unit within a vector can affect the efficiency of gene editing.[5,24,25] To investigate this further, we compared the expression and gene editing efficiency from two single AAV-CRISPR vector designs where Cas9 is driven by the cytomegalovirus intermediate-early enhancer and promoter (CMV-IE) and the gRNA is expressed under the human U6 (hU6) promoter. Both these promoters are short and have strong ubiquitous expression, making them popular choices for all-in-one vectors. In this system, orientation of the gRNA relative to the Cas9 affects both Cas9 and gRNA expression and gene editing efficiency when delivered via AAV. This effect was observed for gRNAs targeting genes involved in the pathogenesis of the eye diseases age-related macular degeneration (Vascular Endothelial Growth Factor, VEGF) and retinitis pigmentosa (Rhodopsin, RHO). This effect, however, was not observed when the Cas9 and gRNA were delivered to cells by transient transfection of plasmids.

Materials and Methods

Plasmid Cloning

The pX601-AAV-CMV-SaCas9-U6-sgRNA plasmid was a gift from Feng Zhang (Addgene plasmid # 61591).[5] The reverse-oriented U6-gRNA plasmid was generated by subcloning with NotI and KpnI (New England Biolabs, UK). gRNAs were subcloned into the BsaI restriction

site. gRNAs used in this study targeted vascular endothelial growth factor (VEGF)[26] and Rhodopsin (RHO) and sequences are listed in the supplementary material. For transfection experiments, endotoxin-free plasmid preparations were created using the EndoFree Plasmid Maxi Kit (Qiagen, UK).

Viral vector production and titration

AAV production and titration was performed as described previously.[27–29] AAV2/2 vectors were created by co-transfection of HEK293T cells seeded in HYPERflasks (Corning, UK) with a PEI protocol to deliver a total of 500 μg of a pDG plasmid containing the required helper and packaging genes (PF421PlasmidFactory, Germany) and the AAV-SaCas9 plasmid. Cells were harvested and lysed 3 days post-transfection. AAV was subsequently isolated by ultracentrifugation with an iodixanol gradient and purified in Amicon Ultra-15 100K filter units (MerckMillipore, UK). SDS-PAGE analysis was used to confirm the purity of each preparation. DNAse resistant particle titering of all vectors was performed in parallel using primers to the bovine growth hormone (bGH) poly-A tail present for all vectors and linearised vector plasmid as a known standard. Primer sets were confirmed to have 90–105% efficiency.

Cell Culture

HEK293 cells (GenTarget Inc, USA) were maintained in complete medium created from High-Glucose Dubecco Modified Eagle Medium (DMEM, Gibco UK) with L-glutamine, supplemented with 10% foetal bovine serum (Gibco, UK, South American origin) and 5% penicillin-streptomycin (Sigma UK). Cells were cultured at 37°C in a 5% CO2 humidified incubator (Thermo Electron). For plasmid transfections, cells were seeded in 24 well plates and were transfected at 24 hours after seeding, when they had reached approximately 80% confluence. Cells were transfected with 500 ng of plasmid DNA together with TransIT-LT1 transfection reagent (Mirus Bio, UK) mixed with OptiMEM serum free media. At 48 hours post-transfection, cells were harvested, divided across two tubes, and frozen for analysis. For AAV transduction experiments, cells were seeded in 12 well plates and were transduced at 24 hours post-seeding when approaching confluency at a multiplicity of infection (MOI) of 300 viral genomes (vg) per cell. At 72 hours post-transduction, cells were harvested, divided across three tubes, and frozen for further analysis.

DNA analysis

Following genomic DNA extraction (QIAamp DNA mini kit, Qiagen), locus PCR of the relevant target (VEGF, RHO) was performed (KOD Hotstart Mastermix, Merck-Millipore,

USA). Products were analysed on an agarose gel to confirm a clean amplification reaction before being sequenced with Sanger sequencing (Eurofins Genomics, Germany). DNA editing efficiency was calculated by uploading chromatograms to the Tracking of Indels by Decomposition (TIDE)[30] online software to calculate indel percentage. Chromatograms from untransfected cells were used as a control. Decomposition windows and left boundaries were optimized to obtain the highest alignment possible. Indel sizes were kept constant at 10. The significance cutoff was maintained at $p < 0.001$ for all analyses.

Transcript analysis

RNA was extracted using the miRNAeasy mini kit (Qiagen, UK) to ensure capture of the small gRNA fragments. RNA was reverse transcribed to cDNA using the Superscript III first strand synthesis system (Thermofisher, UK). 1μg of RNA was reverse transcribed using oligo dT primers and with gene specific primers to the directed repeat region of the SaCas9-gRNA, and cDNA was cleaned in QIAGEN spin columns. Semi-quantitative PCR (qPCR) was performed using Taqman Fast Universal Mastermix (Thermofisher Scientific). Taqman probes measuring expression of *GAPDH* (Hs9999905_m1) and *ACTB* (Hs01060665_g1) were used as endogenous controls and measurement of *SaCas9* and *SaCas9-gRNA* was performed with custom TaqMan probes (Thermofisher Scientific). All assays were validated using dilution series to ensure reaction efficiency of 90-105%. For reactions amplifying the gRNA scaffold, betaine 1X was added to the amplification reaction to reduce secondary structure formation. All qPCR experiments were performed in triplicate in 20 μL reactions on a real-time PCR machine (BioRad). Results were normalised to endogenous controls and presented as a fold change relative to expression from the forward direction using the Livak ($2^{-\Delta\Delta CT}$) method.[31] All primer and probe sequences are listed in the supplementary material.

Western blot

Samples were lysed in RIPA buffer (Merck-Millipore, UK) plus proteasome inhibitor (Roche, UK) using a hand-held homogenizer prior to centrifugation. The Pierce bicinchoninic acid (BCA) protein assay kit (Thermofisher, UK) was used to measure total protein concentration. Samples of 50μg of protein was mixed with 5x protein loading buffer (National Diagnostics, USA) and denatured at room temperature for 15 minutes. Samples and a protein size ladder (BlueEYE, SigmaAldrich, UK) were loaded onto a 10% Tris-Glycine extended gel (Criterion TGX Precast Gel, Biorad, UK) and transferred to a polyvinylidene difluoride membrane using a TransBlotTurbo (BioRad). Membranes were blocked in Odyssey blocking buffer in PBS (LI-COR Biosciences, UK, UK) for one hour, incubated in primary antibody solution with rabbit

anti-SaCas9 (1:10,000, ab203933, Abcam, UK) and mouse anti-alpha-Tubulin (1:5000, ab7291, Abcam, UK) for two hours, and incubated in IRDye fluorescent secondary antibody solution (Donkey anti-rabbit 800W, donkey anti-mouse 680RD, both 1:10,000, LI-COR Biosciences, UK) for one hour. All steps were completed on an orbital shaker at room temperature with washes between each step. Signals were recorded with the Odyssey imaging system and band densities assessed using Image Studio Lite software. SaCas9 levels were normalized to Alpha-tubulin levels and presented as relative to expression from the forward-oriented U6.gRNA constructs.

Statistics

GraphPad Prism (v8) was used for all statistical analysis. Statistics are presented as mean [95% confidence interval. Statistical analysis was performed using a two-way ANOVA with Sidak's post-hoc test for multiple comparisons.

Results

Reverse orientation of the gRNA reduces on-target editing in AAV transduced cells

The smaller Cas9 orthologue of *Staphyloccocus aureus* (SaCas9, 3.2kb) is the most well characterised Cas9 for single AAV delivery. The hU6 promoter is commonly used for high, ubiquitous RNA polymerase III-mediated expression of the gRNA. We cloned plasmid constructs that contained the hU6-gRNA construct in either the forward or reverse direction relative to an upstream SaCas9 driven by the ubiquitous RNA polymerase II-mediated CMV-IE promoter (Fig 1). gRNAs targeting *VEGF* and *RHO* loci were cloned into both the forward and reverse constructs. AAV2 vectors were then created using these constructs.

To investigate the effect of the orientation of the gRNA on *SaCas9* mediated editing, HEK293 cells were either transduced with AAV or transiently transfected with plasmids. In cells transiently transfected with plasmids, no difference in editing rate between constructs with guides oriented in the forward or reverse direction was observed with either the *VEGF* ($p = 0.98$) or *RHO* ($p = 0.98$) guides. In cells transduced with AAV however, editing rates with constructs containing the U6-gRNA in the reverse direction compared to constructs with the gRNA in the forward direction were reduced by 28.7% ($p = 0.0009$) for the *VEGF* guide (Fig 2). A 16.3% ($p = 0.39$) reduction in editing observed for the reverse oriented guide compared to the forward oriented guide targeting the *RHO* locus was not statistically significant.

Reverse orientation of the gRNA reduces Cas9 mRNA and gRNA expression in AAV transduced cells

We hypothesised that the reduced editing rates observed when using the reverse-oriented U6-gRNA promoter in the AAV vector may be due to promoter inhibition of the either the CMV-IE or U6 promoter reducing *SaCas9* or gRNA expression respectively. Thus, expression levels of *SaCas9* mRNA and gRNA were measured using quantitative real-time PCR (qPCR). We found that compared to the forward-oriented vector, the reverse-oriented U6 construct resulted in a significant reduction in *SaCas9* expression in a guide independent manner. A 54% reduction ($p = 0.0005$) in *SaCas9* expression was observed in the *VEGF* targeting constructs and a 44% reduction ($p = 0.023$) was observed in *RHO* targeting constructs when the U6-gRNA complex was reversed compared to the forward direction. A similar, significant reduction in gRNA expression was also found. A reduction of 44% ($p = 0.01$) and 37% ($p = 0.02$) of gRNA expression was seen for the *VEGF* and *RHO* guides respectively when expressed in the reverse relative to the forward direction. In cells transfected with the plasmid construct, no significant effect on SaCas9 or gRNA expression was observed across either gRNA, expressed in either the forward or reverse orientation.

Reverse orientation of the gRNA reduces Cas9 protein expression

To confirm that reduced *SaCas9* mRNA resulted in lower SaCas9 protein expression, we analysed Cas9 expression in the AAV-transduced samples with western blot. For both the *VEGF* and *RHO* guides, *SaCas9* protein expression appeared reduced in constructs with the gRNA in the reverse direction (Fig 3). Using band densitometry, we confirmed that relative to the forward direction, there is a significant reduction in SaCas9 protein when the U6-gRNA cassette is in the reverse compared to forward orientation in both the VEGF construct (62% reduction, $p = 0.0001$) and the RHO construct (30% reduction, $p = 0.001$) (Fig 3). The greater reduction in expression we observed in the reverse-oriented VEGF-targeting construct compared to the RHO-targeting construct is consistent with the greater loss of editing efficiency in the VEGF reverse construct.

Discussion

As gene editing using AAV delivered CRISPR-Cas9 moves towards the clinic,[1] it is important to optimise the design of AAV transgenes to enable therapeutic efficacy. Here, we show that a small change to the transgene design, reversing the direction of the U6 promoter and gRNA complex, has a marked impact on Cas9 and gRNA expression and subsequent editing rates in a vector with SaCas9 driven by the CMV-IE promoter. This effect was only seen once the transgene was packaged and delivered via AAV, not through plasmid transfection. We

demonstrate this finding independently across two different guides. As AAV creation is both time and resource intensive, transgenes are often tested and optimised in plasmid transfection experiments prior to creating AAV. These results indicate that data from experiments using plasmid transfection do not necessarily correlate with those found following AAV transduction.

While there is limited evidence as to how the position and orientation of the U6 promoter in an AAV-CRISPR vector affects gene editing, it is clear that orientation can impact gene editing rates. In the initial characterisation of SaCas9, Friedland et al. packaged two U6-gRNA complexes with D10A SaCas9 nickase in the forward and reverse direction into AAV constructs.[25] Friedland et al. found lower Cas9 expression and editing efficiencies were seen when the U6-gRNA complexes were oriented in the reverse direction. The U6-gRNA cassette in Friedland et al. was located upstream of the Cas9, compared to the downstream location in the present study. Ran et al. evaluated both the *in vitro* and *in vivo* gene editing activity of SaCas9 using a vector expressing SaCas9 and gRNA.[5] The plasmid used in the *in vitro* characterisation (Px601, available from Addgene) has been widely used, including in the present paper, and contains the U6-gRNA in the forward direction.[5] When Ran et al. developed an AAV for the *in vivo* characterisation of SaCas9, however, the AAV transgene contained the U6-gRNA in the reverse direction. No data were presented to compare the activity of the forward and reverse constructs or validate why the U6-gRNA complex was reversed in the AAV vector.[5] Most recently, Levy et al. engineered a dual-AAV split-intein SaCas9 base editor and found that moving the U6-gRNA complex from upstream of the SaCas9 in the forward orientation to downstream in the reverse orientation substantially improved editing rates.[24]

Our data builds on work in other systems that have demonstrated that the arrangement of expression cassettes in a bi-cistronic transgene can affect transgene expression. When a second promoter is added, the activity of both the upstream and downstream promoter was shown to be affected in eukaryotes with lentiviral[19] and transient transfection systems,[20] and in prokaryotes with transient transfection systems.[32] Although each of these studies examined two polymerase II promoters, in the two studies that compared placement of the downstream promoter in reverse compared to a forward direction found the the reverse direction enhanced expression of both promoters.[20,32]

How bi-cistronic constructs are affected also appears to depend on the promoter used, in addition to how they are arranged. For example, an interphotoreceptor retinoid binding protein

promoter suppressed the activity of a rhodopsin kinase promoter, but only when located in the downstream but not the upstream position.[21] Variable results have been found when the U6 promoter is used in combination with other promoters. Placed divergent to a ubiquitin C (UbiC) promoter, U6 promoter activity was inhibited compared to a tandem orientation in a retroviral system.[22] Conversely, when the U6 promoter was paired with a phosphoglycerate kinase (PGK) promoter[22] or another U6 promoter[23] in any orientation, the activity of the U6 promoter was not affected. A lack of agreement between published studies prevents the extrapolation of general rules about the optimal arrangement of promoters for other vectors. This study considers only the combination of the CMV-IE and the hU6 promoter, however it suggests that it is necessary to assess each system and set of promoters in the process of optimising a transgene such as an all-in-one AAV-CRISPR vector.

The underlying mechanisms of our findings remain unknown. In the current study, we observe that the reversal of the RNA-pol III U6 promoter impairs expression from the U6 promoter itself and also a RNA-Pol II CMV-IE promoter upstream in the same construct, but only when expressed in an AAV system. Torsional effects from the unwinding of DNA during active transcription within the AAV episome may be implicated.[33] Transcription from the U6 promoter in the forward direction would result in relaxed negatively supercoiled DNA upstream of the promoter. In contrast, orientation of the downstream U6 promoter in the reverse direction could result in an accumulation of tightly wound positively supercoiled DNA between the cistrons, downstream of both the CMV-IE and U6 promoter; this may stall transcription of both promoters.[32,34]

Transcriptional interference arising from one transcribing RNA polymerase directly impeding another transcribing RNA polymerase[35] may also play a role. Following AAV transduction, AAV genomes form double-stranded episomal circular monomers and concatemers, where viral transgenes form linked circles connected by ITRs.[36,37] Within the circular episome, the transgenes can be linked to one another in any direction, 5'-3' or 3'-5'. For a given transgene, there are three possible arrangements (Fig 4). In the vectors containing the U6-gRNA in the forward orientation relative to the Cas9, only one of these combinations places two promoters directly adjacent to one another, separated by ITRs. In the vectors containing the U6-gRNA in the reverse orientation relative to the Cas9 however, in all possible arrangements, the promoters are directly adjacent to one another. This is the case whether the U6-gRNA is located upstream[25] or downstream of the Cas9 cassette. The closer physical proximity of both the polymerase II and

III promoters in the concatemers when the gRNA is in the reverse direction may increase the susceptibility of expression from these promoters being affected by transcriptional interference and local torsional effects of transcription. ITRs are known to possess promoter activity,[38] and the reverse orientation also places both promoters immediately adjacent to the ITRs in the concatemer. In plasmid transfection, the plasmid backbone is maintained and separates the ends of the transgene and formation of transgene monomers and concatemers does not occur. This model may explain the observed differences in expression between plasmid transfection and AAV transduction.

Conclusion

Our study highlights two key points. Firstly, for the design of all-in-one AAV-CRISPR vectors, it is important to consider the orientation of promoters within the transgene when optimising transgene expression. This effect has been seen using the CMV-IE and hU6 promoter in vitro. Expression is likely to be promoter dependent, further work is needed to test different vector designs across different tissue types, including in vivo. This includes further evaluation of other promoters like a cell-specific promoter for each specific application. Secondly, this study suggests that this testing and optimisation should be done with AAV vectors, as results found from plasmid transfection may not translate to those found with AAV vectors.

Acknowledgements

This research was funded by support from the NIHR Oxford Biomedical Research Centre, the Rhodes Trust, the North Harbour Club Charitable Trust and the Amar-Franses & Foster-Jenkins Trust.

Figures

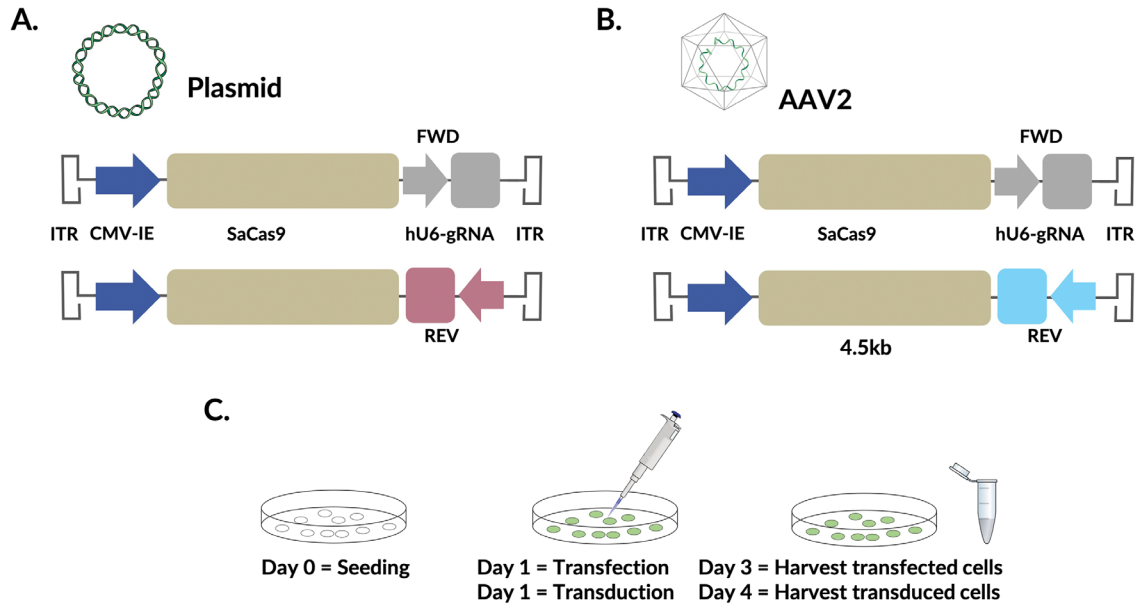

Figure 1 | A. Vector diagram of the forward and reverse oriented U6-gRNA promoter plasmids used for transient transfection. B. Vector diagram of the forward- and reverse-oriented U6-gRNA promoter AAV vectors used for transduction. C. Outline of transfection and transduction protocols.

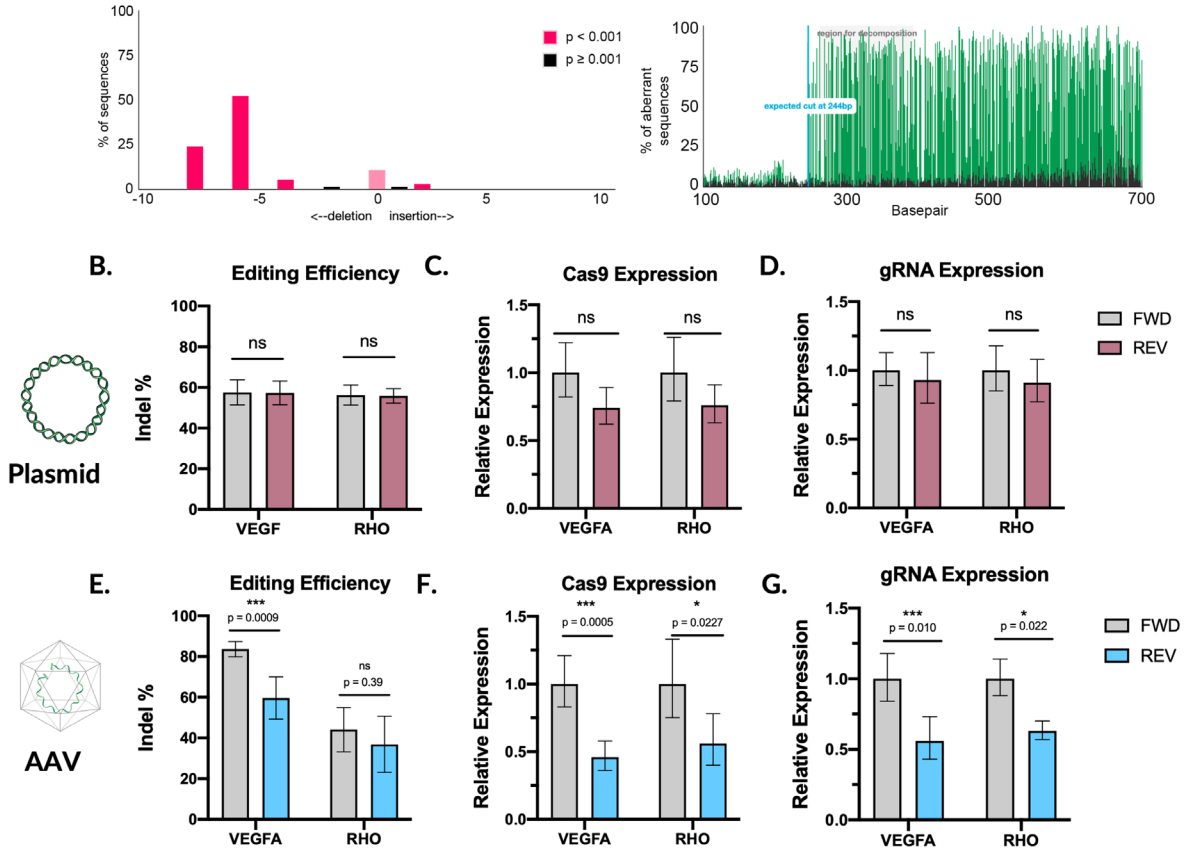

Figure 2 | A. Representative example of a TIDE analysis output analysing indels in a sequencing chromatogram from samples transduced with vectors targeting *VEGF*. **B**. On-target editing efficiency in plasmid-transfected samples for guides targeting *VEGF* (Forward = 57.6% [51.4, 63.8], Reverse = 57.2% [51.4, 63.1], p = 0.98, n = 6) and *RHO* (Forward = 56.2% [51.3, 61.2], Reverse = 56.7% [52.2, 59.3], p = 0.98, n = 6) **C.** *SaCas9* mRNA expression from plasmid transfected samples (VEGF-Rev = 0.74 [0.62, 0.89], p = 0.13, n = 5) and *RHO* (RHO-Rev = 0.76 [0.63, 0.91], p = 0.12, n = 6). **D.** gRNA expression from plasmid transfected samples (VEGF-Rev = 0.93 [0.76, 1.13], p = 0.80, n = 5) and RHO (RHO-Rev = 0.91 [0.77, 1.08], p = 0.67, n = 6). **E**. On-target editing efficiency in AAV transduced cells as assessed by TIDE analysis for the *VEGF* gRNA (Forward = 87.2% [79.8, 87.2], Reverse = 59.6% [49.2, 70.0], p = 0.0009, n = 6) and the *RHO* gRNA (Forward = 44.0% [33.2, 54.9], Reverse = 36.8% [23.1, 50.6], p = 0.39, n = 6). **F**. *SaCas9* expression in AAV transduced cells (VEGF-Rev = 0.46 [0.36, 0.58], p = 0.0005, n = 6; RHO-Rev = 0.56 [0.40, 0.78], p = 0.023, n = 4). **G.** gRNA expression assessed in AAV transduced cells (VEGF-Rev = 0.56 [0.43, 0.73], p = 0.01, n = 6; RHO-Rev = 0.63 [0.57, 0.70], p = 0.02, n = 4). Data presented as mean [95% CI], two-way unpaired ANOVA with Sidak's multiple comparison testing. *SaCas9* and gRNA expression calculated as fold change relative to the forward oriented gRNA.

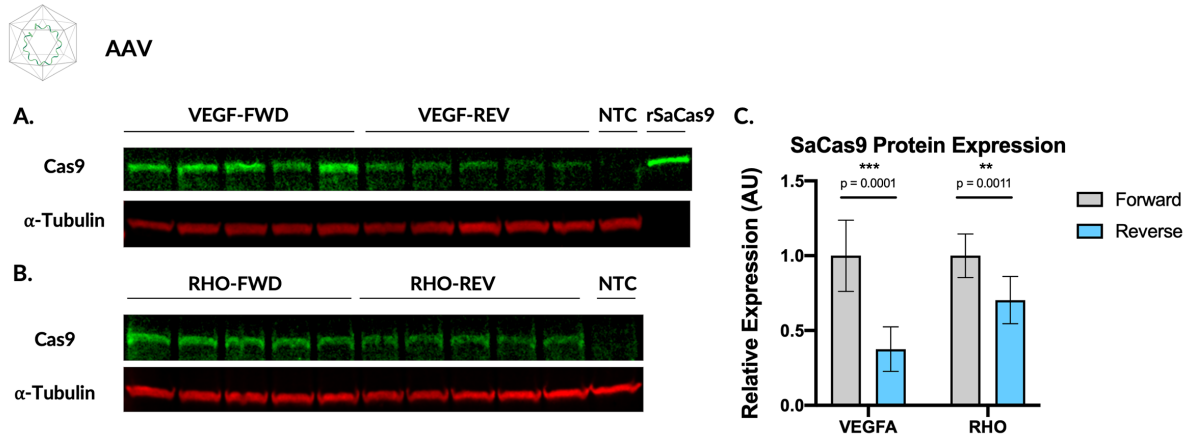

Figure 3 | **A**. Western blot of AAV transduced samples targeting VEGF. **B**. Western blot of AAV-transduced samples targeting RHO. **C**. Quantitative analysis of band densities normalised to alpha-Tubulin, relative to the expression of SaCas9 with U6 in the forward orientation. (VEGF-Rev = 0.38 [0.23, 0.52], p = 0.0001, n = 5; RHO-Rev = 0.70 [0.54, 0.86], p = 0.001, n = 5). Data presented as mean ± 95% CI, two-way unpaired ANOVA with Sidak's multiple comparison testing. NTC = non transfected control, rSaCas9 = 100ng recombinant SaCas9 protein.

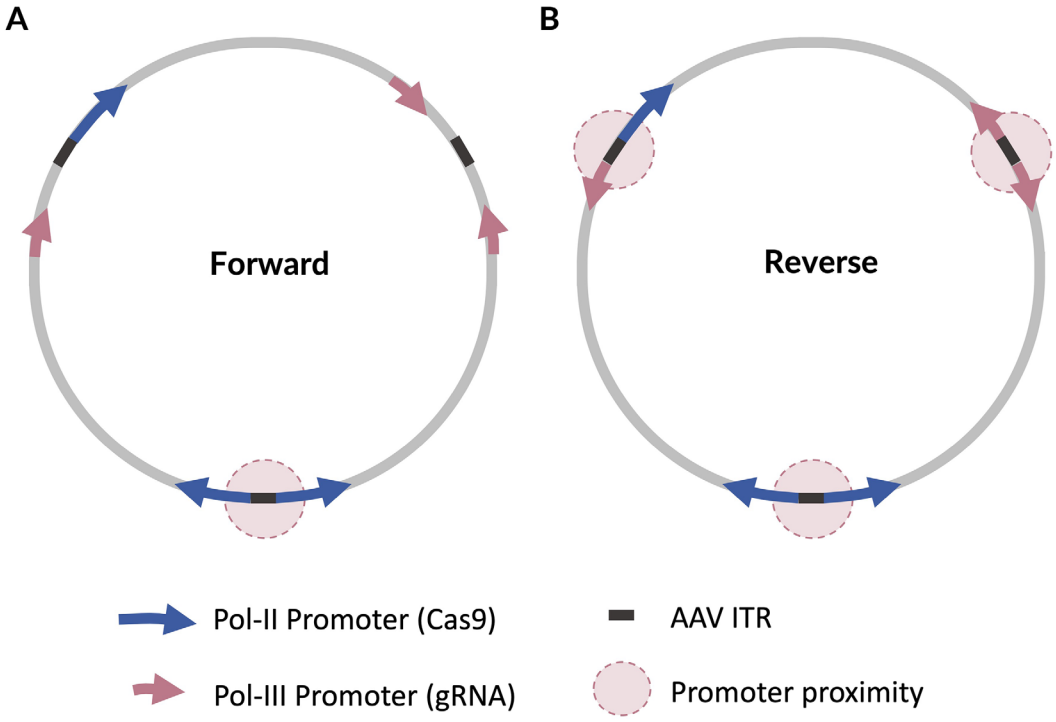

Figure 4 | A model of the three possible arrangements of a dual-transgene containing Cas9 driven by a Pol-II promoter and a gRNA driven by a Pol-III promoter in a circular episomal monomer or concatemer. **A.** With the gRNA and its promoter is oriented in the forward direction, in only one conformation of transgene concatemer results in promoter proximity. **B.** In concatemers with the gRNA and its promoter oriented in the reverse direction, all conformations of the transgene concatemer result in proximity between the promoters.

References

1. Maeder ML, Stefanidakis M, Wilson CJ, et al. Development of a gene-editing approach to restore vision loss in Leber congenital amaurosis type 10. *Nat Med*. 2019;25:229–33. DOI: 10.1038/s41591-018-0327-9.
2. Xue K, Jolly JK, Barnard AR, et al. Beneficial effects on vision in patients undergoing retinal gene therapy for choroideremia. *Nat Med*. 2018;24:1507–12. DOI: 10.1038/s41591-018-0185-5.
3. Cehajic-Kapetanovic J, Xue K, Martinez-Fernandez de la Camara C, et al. Initial results from a first-in-human gene therapy trial on X-linked retinitis pigmentosa caused by mutations in RPGR. *Nat Med*. 2020. DOI: 10.1038/s41591-020-0763-1.
4. Russell S, Bennett J, Wellman JA, et al. Efficacy and safety of voretigene neparvovec (AAV2-hRPE65v2) in patients with RPE65 -mediated inherited retinal dystrophy: a randomised, controlled, open-label, phase 3 trial. *Lancet*. 2017;390:849–60. DOI: 10.1016/S0140-6736(17)31868-8.
5. Ran FA, Cong L, Yan WX, et al. In vivo genome editing using Staphylococcus aureus Cas9. *Nature*. 2015;520:186–91. DOI: 10.1038/nature14299.
6. Li A, Lee CM, Hurley AE, et al. A Self-Deleting AAV-CRISPR System for In Vivo Genome Editing. *Mol Ther - Methods Clin Dev*. 2019;12:111–22. DOI: 10.1016/j.omtm.2018.11.009.
7. Yang Y, Wang L, Bell P, et al. A dual AAV system enables the Cas9-mediated correction of a metabolic liver disease in newborn mice. *Nat Biotechnol*. 2016;34:334–8. DOI: 10.1038/nbt.3469.
8. Jarrett KE, Lee CM, Yeh Y-H, et al. Somatic genome editing with CRISPR/Cas9 generates and corrects a metabolic disease. *Sci Rep*. 2017;7:44624. DOI: 10.1038/srep44624.
9. Yu W, Mookherjee S, Chaitankar V, et al. Nrl knockdown by AAV-delivered CRISPR/Cas9 prevents retinal degeneration in mice. *Nat Commun*. 2017;8:14716. DOI: 10.1038/ncomms14716.
10. Kim E, Koo T, Park SW, et al. In vivo genome editing with a small Cas9 orthologue derived from Campylobacter jejuni. *Nat Commun*. 2017;8:1–12. DOI: 10.1038/ncomms14500.
11. Hung SSC, Chrysostomou V, Li F, et al. AAV-Mediated CRISPR/Cas Gene Editing of Retinal Cells In Vivo. *Investig Opthalmology Vis Sci*. 2016;57:3470–6. DOI: 10.1167/iovs.16-19316.
12. Tsai YT, Wu WH, Lee TT, et al. Clustered Regularly Interspaced Short Palindromic Repeats-Based Genome Surgery for the Treatment of Autosomal Dominant Retinitis Pigmentosa. *Ophthalmology*. 2018;125:1421–30. DOI: 10.1016/j.ophtha.2018.04.001.
13. Murlidharan G, Sakamoto K, Rao L, et al. CNS-restricted Transduction and CRISPR/Cas9-mediated Gene Deletion with an Engineered AAV Vector. *Mol Ther - Nucleic Acids*. 2016;5:e338. DOI: 10.1038/mtna.2016.49.
14. Guo Y, VanDusen NJ, Zhang L, et al. Analysis of Cardiac Myocyte Maturation Using CASAAV, a Platform for Rapid Dissection of Cardiac Myocyte Gene Function In Vivo. *Circ Res*. 2017;120:1874–88. DOI: 10.1161/CIRCRESAHA.116.310283.
15. Ishizu T, Higo S, Masumura Y, et al. Targeted Genome Replacement via Homology-directed Repair in Non-dividing Cardiomyocytes. *Sci Rep*. 2017;7:9363. DOI: 10.1038/s41598-017-09716-x.
16. Tabebordbar M, Zhu K, Cheng JKW, et al. In vivo gene editing in dystrophic mouse muscle and muscle stem cells. *Science*. 2016;351:407–11. DOI: 10.1126/science.aad5177.
17. Nelson CE, Hakim CH, Ousterout DG, et al. In vivo genome editing improves muscle function in a mouse model of Duchenne muscular dystrophy. *Science*. 2016;351:403–7. DOI: 10.1126/science.aad5143.

18. Long C, Amoasii L, Mireault AA, et al. Postnatal genome editing partially restores dystrophin expression in a mouse model of muscular dystrophy. *Science*. 2016;351:400–3. DOI: 10.1126/science.aad5725.
19. Curtin JA, Dane AP, Swanson A, et al. Bidirectional promoter interference between two widely used internal heterologous promoters in a late-generation lentiviral construct. *Gene Ther*. 2008;15:384–90. DOI: 10.1038/sj.gt.3303105.
20. Park SK, Hwang BJ, Kee Y. Promoter cross-talk affects the inducible expression of intronic shRNAs from the tetracycline response element. *Genes and Genomics*. 2019;0:0. DOI: 10.1007/s13258-019-00784-z.
21. Semple-Rowland SL, Coggin WE, Geesey M, et al. Expression characteristics of dual-promoter lentiviral vectors targeting retinal photoreceptors and Müller cells. *Mol Vis*. 2010;16:916–34.
22. Nie L, Thakur M Das, Wang Y, et al. Regulation of U6 Promoter Activity by Transcriptional Interference in Viral Vector-Based RNAi. *Genomics, Proteomics Bioinforma*. 2010;8:170–9. DOI: 10.1016/S1672-0229(10)60019-8.
23. Lambeth LS, Van Hateren NJ, Wilson SA, et al. A direct comparison of strategies for combinatorial RNA interference. *BMC Mol Biol*. 2010;11:77. DOI: 10.1186/1471-2199-11-77.
24. Levy JM, Yeh W-H, Pendse N, et al. Cytosine and adenine base editing of the brain, liver, retina, heart and skeletal muscle of mice via adeno-associated viruses. *Nat Biomed Eng*. 2020;4:97–110. DOI: 10.1038/s41551-019-0501-5.
25. Friedland AE, Baral R, Singhal P, et al. Characterization of Staphylococcus aureus Cas9: a smaller Cas9 for all-in-one adeno-associated virus delivery and paired nickase applications. *Genome Biol*. 2015:1–10. DOI: 10.1186/s13059-015-0817-8.
26. Kleinstiver BP, Prew MS, Tsai SQ, et al. Engineered CRISPR-Cas9 nucleases with altered PAM specificities. *Nature*. 2015;523:481–5. DOI: 10.1038/nature14592.
27. McClements ME, Barnard AR, Singh MS, et al. An AAV Dual Vector Strategy Ameliorates the Stargardt Phenotype in Adult Abca4 −/− Mice. *Hum Gene Ther*. 2019;30:590–600. DOI: 10.1089/hum.2018.156.
28. Lipinski DM, Barnard AR, Singh MS, et al. CNTF Gene Therapy Confers Lifelong Neuroprotection in a Mouse Model of Human Retinitis Pigmentosa. *Mol Ther*. 2015;23:1308–19. DOI: 10.1038/mt.2015.68.
29. Fischer MD, McClements ME, Martinez-Fernandez de la Camara C, et al. Codon-Optimized RPGR Improves Stability and Efficacy of AAV8 Gene Therapy in Two Mouse Models of X-Linked Retinitis Pigmentosa. *Mol Ther*. 2017;25:1854–65. DOI: 10.1016/j.ymthe.2017.05.005.
30. Brinkman EK, Chen T, Amendola M, et al. Easy quantitative assessment of genome editing by sequence trace decomposition. *Nucleic Acids Res*. 2014;42:e168–e168. DOI: 10.1093/nar/gku936.
31. Livak KJ, Schmittgen TD. Analysis of Relative Gene Expression Data Using Real-Time Quantitative PCR and the $2^{-\Delta\Delta CT}$ Method. *Methods*. 2001;25:402–8. DOI: 10.1006/meth.2001.1262.
32. Yeung E, Dy AJ, Martin KB, et al. Biophysical Constraints Arising from Compositional Context in Synthetic Gene Networks. *Cell Syst*. 2017;5:11-24.e12. DOI: 10.1016/j.cels.2017.06.001.
33. Ma J, Bai L, Wang MD. Transcription under torsion. *Science*. 2013;340:1580–3. DOI: 10.1126/science.1235441.
34. Kouzine F, Liu J, Sanford S, et al. The dynamic response of upstream DNA to transcription-generated torsional stress. *Nat Struct Mol Biol*. 2004;11:1092–100. DOI: 10.1038/nsmb848.
35. Shearwin KE, Callen BP, Egan JB. Transcriptional interference - A crash course. *Trends*

Genet. 2005;21:339–45. DOI: 10.1016/j.tig.2005.04.009.
36. Penaud-Budloo M, Le Guiner C, Nowrouzi A, et al. Adeno-Associated Virus Vector Genomes Persist as Episomal Chromatin in Primate Muscle. *J Virol*. 2008;82:7875–85. DOI: 10.1128/JVI.00649-08.
37. Nakai H, Yant SR, Storm TA, et al. Extrachromosomal Recombinant Adeno-Associated Virus Vector Genomes Are Primarily Responsible for Stable Liver Transduction In Vivo. *J Virol*. 2001;75:6969–76. DOI: 10.1128/jvi.75.15.6969-6976.2001.
38. Yan Z, Sun X, Feng Z, et al. Optimization of Recombinant Adeno-Associated Virus-Mediated Expression for Large Transgenes, Using a Synthetic Promoter and Tandem Array Enhancers. *Hum Gene Ther*. 2015;26:334–46. DOI: 10.1089/hum.2015.001.